



HAL
open science

Application of Regularized Digital Images Correlation Analysis to the Tensile Test of NiTi Shape Memory Alloy

Xuyang Chang, Mame Daro Fall, Karine Lavernhe Taillard, Olivier Hubert

► **To cite this version:**

Xuyang Chang, Mame Daro Fall, Karine Lavernhe Taillard, Olivier Hubert. Application of Regularized Digital Images Correlation Analysis to the Tensile Test of NiTi Shape Memory Alloy: Application de la corrélation d'images régularisé pour 1D tensile test sur l'alliage à mémoire de forme type NiTi. 23ème Congrès Français de Mécanique 2017, Aug 2017, Lille, France. hal-01559845

HAL Id: hal-01559845

<https://hal.science/hal-01559845>

Submitted on 11 Jul 2017

HAL is a multi-disciplinary open access archive for the deposit and dissemination of scientific research documents, whether they are published or not. The documents may come from teaching and research institutions in France or abroad, or from public or private research centers.

L'archive ouverte pluridisciplinaire **HAL**, est destinée au dépôt et à la diffusion de documents scientifiques de niveau recherche, publiés ou non, émanant des établissements d'enseignement et de recherche français ou étrangers, des laboratoires publics ou privés.

Application of Regularized Digital Images Correlation Analysis to the Tensile Test of NiTi Shape Memory Alloy

X. Chang, M. D. Fall, K. Lavernhe-Taillard, O. Hubert

LMT (ENS-Paris-Saclay / CNRS / Université Paris-Saclay)
61 Avenue du président Wilson, France, 94235, Cachan Cedex
chang@lmt.ens-cachan.fr

Abstract :

Shape Memory Alloys (SMA) undergo an austenite-martensite solid-solid phase transformation which confers its super-elastic and shape memory behaviors. Phase transformation can be induced either by stress or temperature changes, thus indicating a strong thermomechanical coupling. Until now, the increasing use of SMA for complex applications requires a robust multiphysic and multiaxial modeling of phenomena governing their behaviors.

1D tensile loading test is applied to a small strip specimen made of NiTi SMA (Ni 49.8 at%). During the tensile test, phase transformation of SMA occurs in the form of strain localization bands. Despite the progress in Digital Images Correlation techniques (DIC), the measurement of strain localization remains challenging for small size samples addressed in this study. It is shown how the introduction of the Regularized Digital Images Correlation (R-DIC) is relevant for such measurement by offering a better spatial resolution and shorter computation times.

Key words : Shape Memory Alloy (SMA), Thermomechanical Coupling, Digital images correlation (DIC)

1 Introduction

Shape Memory Alloys (SMA) have nowadays widely industrial applications in multiple fields such as aerospace, civil-engineering, automotive and also in bio-medical area. Their main interests lie in the ability to have very large elastic strain threshold and also the ability to recover from permanent strain after unloading by applying simple heating-cooling treatment (shape recovery up to 10% strain). Meanwhile, it is worth mentioning that there are two different thermomechanical phenomena which makes their own contributions : the so-called shape memory effect and the super-elastic behaviors. These behaviors are the consequences of a specific solid-solid phase transformation which involves a stable phase at high temperature called *austenite* (A) and a stable phase called *martensite* (M) at low temperature. In the macroscopic scale, phase transformation occurs in the form of localization bands [Sun and He (2008) and Maynadier et al. (2014)].

The distribution of *martensite*, *austenite* and possible *R* phases inside, outside the band and at the interface remains meanwhile unknown but would be of great interest for the validation of constitutive laws

[Maynadier et al. (2014)]. Digital Images Correlation analysis (DIC) is an interesting tool to capture the macroscopic strain field during the loading process. On the other hand, in-situ X-ray diffraction analysis is required to measure the local phase ratio inside and outside the transformation band. These experiments are made using small size samples where usual DIC analysis does not permit to reach a sufficient spatial resolution. It is shown in this paper how the introduction of the so-called *Regularized Digital Images Correlation* (R-DIC) leads to a better spatial resolution and shorter computation times. This technique is applied to observe the nucleation and propagation of localization bands in an equiatomic NiTi SMA specimen tensile strained at the room temperature.

2 Regularized Digital Images Correlations

This section is a brief summary of the work by Zvonimir et al. (2013)

2.1 Principles

The sample being observed with a telecentric lens, has a physical size of $56.25 \mu\text{m}^2$ for each pixel. We assume that between the image f in the reference configuration and g in the deformed configuration the gray level is conserved :

$$f(\mathbf{x}) = g(\mathbf{x} + \mathbf{u}(\mathbf{x})) \quad (1)$$

where \mathbf{u} is the displacement field in the deformed configuration. The sought displacement field should minimize the sum of squared difference Φ_c^2 over the chosen area which we called *Region Of Interest* (ROI) :

$$u(\mathbf{x}) = \operatorname{argmin}(\Phi_c^2) \quad (2)$$

where Φ_c^2 is the *correlation residual*:

$$\Phi_c^2 = \int_{ROI} \varphi_c^2(\mathbf{x}) dx \quad (3)$$

here $\varphi_c(\mathbf{x})$ defines the field of correlation residuals:

$$\varphi_c(\mathbf{x}) = |g(\mathbf{x} + \mathbf{u}(\mathbf{x})) - f(\mathbf{x})| \quad (4)$$

As shown in Equation 2 and Equation 3 , this minimization problem is both non-linear and ill-posed since there are two unknowns for a gray level difference, thus it is nearly impossible to determine independently the displacement for each pixel. The solution is to choose a weak formulation (like a Galerkin method in Finite Element Method) in which the displacement field is expressed in multiple sub-domain as :

$$\mathbf{u}(\mathbf{x}) = \sum_n u_n \varphi_n(\mathbf{x}) \quad (5)$$

where φ_n are the vector of sub-fields and u_n are the associated degrees of freedom. Accordingly instead of searching the 'real' minimum of the residual field, we aim to find the 'approached' minimum of the Φ_c^2 with the respect to the unknown u_n in the sense of Finite Element interpolation. The following linear

systems are solved iteratively :

$$[\mathbf{M}]\{\delta\mathbf{u}\} = \{\mathbf{b}\} \quad (6)$$

where $[\mathbf{M}]$ is the correlation matrix formed from the dyadic product of the fields $\nabla f \cdot \varphi_n$ [Hild and Roux (2012)], $\{\mathbf{b}\}$ is a vector that vanishes when a perfect fit is obtained for each pixel (Equation 1 is satisfied), and $\{\delta\mathbf{u}\}$ collects the displacement corrections to the measured degrees of freedom u_n . This approach is the so-called global approach of Digital Images Correlations [Hild and Roux (2012)].

As mentioned in the section of the introduction, in order to capture the evolution of the strain localization bands in a very small specimen, we sometimes need to implement a very fine mesh to achieve a very small scale for spatial resolution. However, based on the nature of the non linear and ill-posed minimization problem, we are very likely to encounter the second minimum trapping problem. The solution is to enforce the mechanical admissibility in the sense of Finite Elements (*FE*) interpolations. Consequently the notion of *Equilibrium Gap* is introduced. Here the isotropic linear elastic behavior is implemented, thus the equilibrium equation writes as :

$$[\mathbf{K}]\{\mathbf{u}\} = \{\mathbf{f}\} \quad (7)$$

where $[\mathbf{K}]$ is the stiffness matrix, $\{\mathbf{f}\}$ the vector of nodal forces (or Generalized force $\{\mathbf{f}\} = \{\mathbf{f}_{\text{ext}}\} + \{\mathbf{f}_{\text{int}}\}$). In the absence of body force, interior nodes of *Region of Interest* are free of any external load $\{\mathbf{f}_{\text{ext}}\} = \mathbf{0}$. When a non-exact displacement vector $\{\mathbf{u}'\}$ is calculated through the Global Digital Images Correlation, the internal force residuals $\{\mathbf{f}_r\} = [\mathbf{K}]\{\mathbf{u}'\} - \{\mathbf{f}\}$ will rise significantly if the displacement field $\{\mathbf{u}\}$ does not satisfy the mechanical equilibrium. Thus a corresponding *equilibrium gap* will appear. The so called *equilibrium gap* method consists of minimizing the mechanical residuals in the *Finite Element* sense:

$$\Phi_m^2 = \{\mathbf{u}\}^t [\mathbf{K}] [\mathbf{K}]^t \{\mathbf{u}\} \quad (8)$$

where t is the transposition operator for the matrix and Φ_m^2 is the sum of equilibrium gap at internal nodes of *Region of Interest*. Additionally, this method requires a supplementary regularization for the boundary nodes of *Region of Interest*. The additional regularization is help to vanish any rigid body motion for the *Region of Interest*.

$$\Phi_b^2 = \{\mathbf{u}\}^t [\mathbf{L}] [\mathbf{L}]^t \{\mathbf{u}\} \quad (9)$$

$[\mathbf{L}]$ is an operator acting only at the boundary nodes and Φ_b^2 is the corresponding *boundary fluctuations*. The construction of the new operator $[\mathbf{L}]$ is detailed in the article of Zvonimir et al. (2013).

2.2 Correlation Procedure

These three different residual terms (*Correlation Residual* Φ_c^2 , *Equilibrium Gap* Φ_m^2 and *Boundary Fluctuations* Φ_b^2) are expressed in different units, thus can be combined into a new residual function Φ_t (*total normalized residual term*) by a proper normalization procedure :

$$(1 + w_m + w_b)\Phi_t^2(v) = \tilde{\Phi}_c^2 + w_m \tilde{\Phi}_m^2 + w_b \tilde{\Phi}_b^2 \quad (10)$$

where w_m and w_b are weights that define length scales associated with $\tilde{\Phi}_m^2$ and $\tilde{\Phi}_b^2$. To perform the procedure of normalization, we use a displacement field in the form of a plane wave $\mathbf{v}(\mathbf{x}) = \mathbf{v}_0 \exp(i\mathbf{k} \cdot \mathbf{x})$ where \mathbf{v}_0 is the amplitude of the wave and \mathbf{k} is the corresponding wave vector. With this choice, the normalized residuals become :

$$\tilde{\Phi}_c^2(v) = \frac{\Phi_c^2}{\{\mathbf{v}\}^t [\mathbf{M}] \{\mathbf{v}\}}, \tilde{\Phi}_m^2(v) = \frac{\Phi_m^2}{\{\mathbf{v}\}^t [\mathbf{K}] [\mathbf{K}]^t \{\mathbf{v}\}}, \tilde{\Phi}_b^2(v) = \frac{\Phi_b^2}{\{\mathbf{v}\}^t [\mathbf{L}] [\mathbf{L}]^t \{\mathbf{v}\}} \quad (11)$$

And the weight w_m and w_b are chosen as

$$w_m = (2\pi |\mathbf{k}| l_m)^4, w_b = (2\pi |\mathbf{k}| l_b)^4 \quad (12)$$

l_m and l_b denote respectively the regularization length for Φ_m^2 and Φ_b^2 .

For example, if $l_m = l_b = \frac{1}{(2\pi)}k$, we verify that $\tilde{\Phi}_c^2(v) = \tilde{\Phi}_m^2(v) = \tilde{\Phi}_b^2(v) = 1$ and $\Phi_t^2(v) = 1$

The normalization term of correlation residual is wave-length independent but the two other normalization terms rise significantly with the wave length $\{\mathbf{k}\}$ [Zvonimir et al. (2013)]. In this way we could consider the total residual function to be a low-frequency pass filter that damps all the deviations of displacement field $\{\mathbf{u}\}$ which are unsatisfying regarding to the mechanical admissibility. By varying the chosen regularization length l_m and l_b , we could choose to filter any potential oscillations above certain value of wave length $\{\mathbf{k}\}$.

The actual limitation comes from the naive assumption of uniform stiffness matrix for the whole ROI region, which is generally untrue for non linear mechanical behaviors. This limitation will be more clearly presented in the next section where a 1D tensile test of a NiTi SMA sample is considered. However, *let us insist that* this regularization does not necessarily imply that the solid is a linear elastic behavior or could accurately be described by the constitutive law for linear elastic material. By placing smaller weight over the mechanical residuals, we assume that the mechanical regularization will not disturb the strain field calculation to a significant level.

2.3 Implementation

Since in most cases the correlation residuals is a non linear function depending on the degrees of freedom in **ROI**, a Newton method iterative procedure is introduced to handle with the non-linear aspect of the minimization problem. By adopting small increment $\{\mathbf{du}\} = \{\mathbf{u}^{j+1}\} - \{\mathbf{u}^j\}$ of the previous solution, the calculation is recast in a matrix-vector product ;

$$([\mathbf{M}] + [\mathbf{N}]) \{\mathbf{du}\} = \{\mathbf{b}\}^j - [\mathbf{N}] \{\mathbf{u}\}^j \quad (13)$$

with

$$[\mathbf{N}] = w_m \frac{\{\mathbf{v}\}^t [\mathbf{M}] \{\mathbf{v}\}}{\{\mathbf{v}\}^t [\mathbf{K}] [\mathbf{K}]^t \{\mathbf{v}\}} [\mathbf{K}]^t [\mathbf{K}] + w_b \frac{\{\mathbf{v}\}^t [\mathbf{M}] \{\mathbf{v}\}}{\{\mathbf{v}\}^t [\mathbf{L}] [\mathbf{L}]^t \{\mathbf{v}\}} [\mathbf{L}]^t [\mathbf{L}] \quad (14)$$

For each iteration j , the picture in the deformed configuration is corrected by using the current estimate of the displacement $\{\mathbf{u}^j\}$. Then the vector $\{\mathbf{b}\}^j$ is accordingly updated. The correlation matrix $[\mathbf{M}]$ and the stiffness matrix $[\mathbf{N}]$ are computed only once for all the iterations. Iterations stop when the displacement correction $\{\mathbf{du}\}$ is smaller than the convergence criteria chosen by the user. At this stage, we assume that the solution $\{\mathbf{u}\}$ has converged.

$$\frac{\partial \Phi_I^2}{\partial u^j} = \{0\} \quad (15)$$

3 Experiments

1D tensile test of a very small *NiTi* (*Ni* 49.8%*at*) strip sample is carried out at room temperature. Regularized Digital Images Correlation analysis is performed to capture the axial strain field.

3.1 Experiment Setup

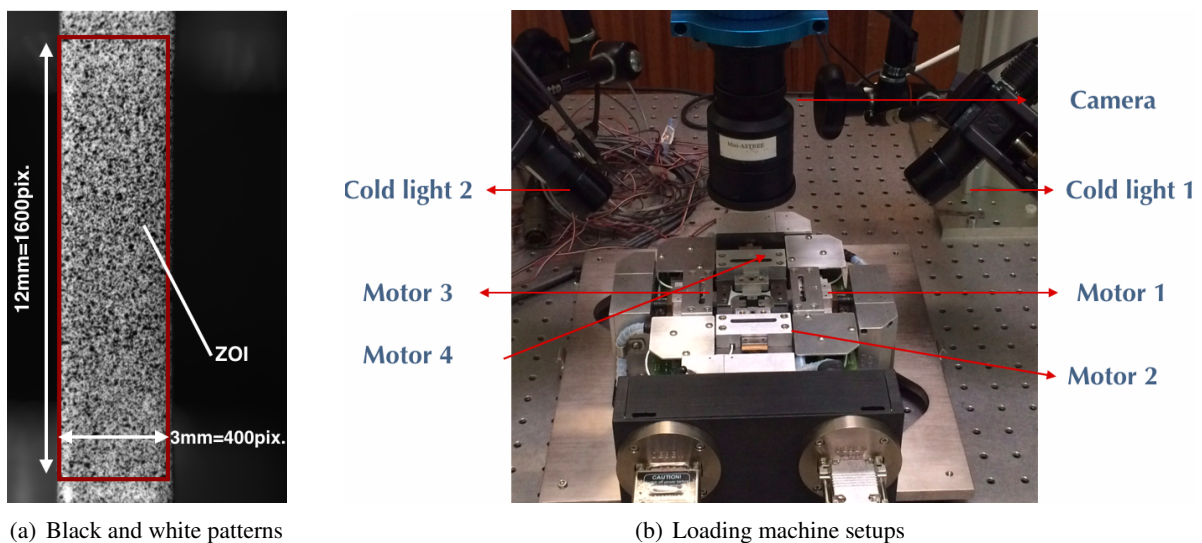
3.1.1 1D sample

A textured poly-crystalline NiTi specimen is considered. The 1D strip specimen is a thin plate with a thickness $e = 0.3$ mm in the zone of interest with a rectangular shape : length = 10 mm, width = 3 mm. This specific design permits to avoid the local heat accumulation due to the phase transformation during the loading process.

In its zone of interest (ZOI), the sample's surface is covered by a black and white speckle pattern made of **Double internal mix airbrush** (see Figure 1.a). The presence of the black and white pattern increases the gray level contrast inside the image. This condition is essential to conduct any accurate Digital Images Correlation analysis.

3.1.2 Loading machine Setups

A small uni-axial machine is used to apply the mechanical loading to the specimen. 2 independent motors are fixed with the specimen with a maximum force up to 2 kN. The specimen is lighted by two cold sources (LED) which are placed in symmetric position to provide a homogeneous lightening condition over the surface of the sample. Camera is placed above and facing perpendicularly the specimen and takes a picture with a controlled frequency during the tensile test (Figure 1.b).



(a) Black and white patterns

(b) Loading machine setups

Figure 1: Experimental setups

3.2 Scale Effect of Regularization Length

On a sample strained at a 1.3% level, Figure 2 illustrates the scale effect with different regularization length chosen : if we take a really low regularization length ($l_m = 10$ pix), the low-frequency pass filter has few impact (every deviation is allowed). Consequently, we will encounter the second minimum trapping problem because of the nature of non-linear and ill-posed formulation for the analysis. As the result, the strain field is filled with noise (Figure 2.c).

If we take a very strong regularization penalty $l_m = 1000$ pix, all the deviation that are not mechanically admissible are damped. Consequently local details of strain field are largely lost (Figure 2.a).

On the contrary, if a proper regularization length $l_m = 100$ pix is chosen for the R-DIC, large deviations that are not mechanically admissible are damped, meanwhile, the details of local strain field are conserved (as shown in Figure 2.b).

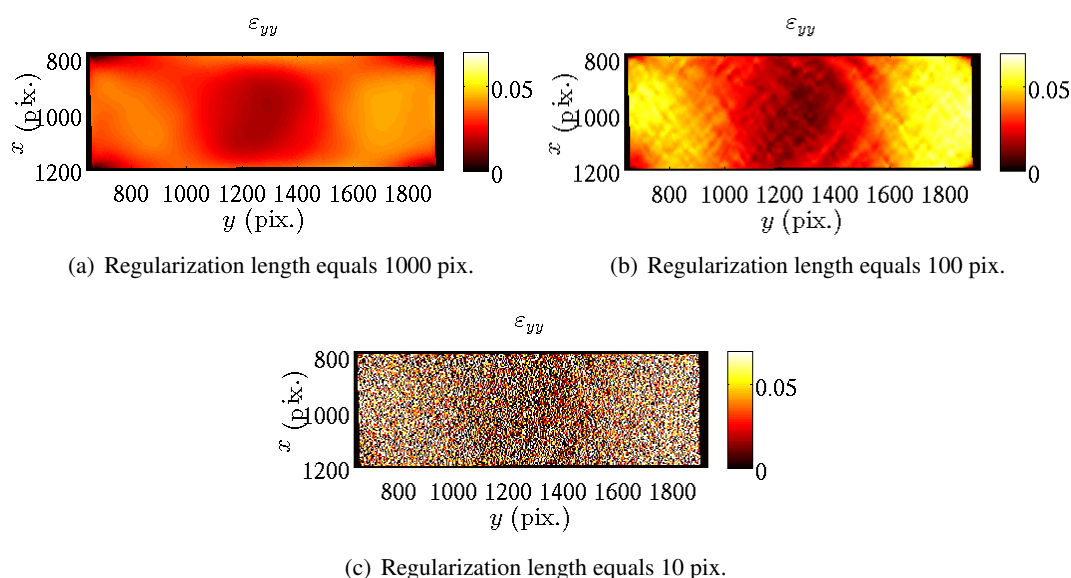


Figure 2: The scale effect of regularization length

3.3 Quasi-static 1D Tensile Test

The 1D tensile loading process is displacement-controlled : the central point of the specimen is kept fixed, consequently greatly vanishing the rigid body motion. A quasi-static tensile test is performed at the room temperature (strain rate $\dot{\epsilon}_{yy} = 0.025\%/s$). The corresponding stress strain curve is plotted in Figure 4. Stress is calculated from the applied force and initial active section. Strain is the mean value over the *region of Interest* calculated by R-DIC analysis : *Region of Interest* has been meshed by 8 pix T3 Element, which offers a spatial resolution of $60\mu\text{m}$. Between each image frame, we have a total residual less than 1.2%.

Here a *relaxation approach* is adopted : each time a first calculation is carried out between the initial image and the deformed image with a chosen regularization length $l_m = 1000$ pix. The following calculations are conducted with a decreasing regularization length until $l_m = 100$ pix. This approach will greatly reduce the computation time compared to a R-DIC analysis with only a single regularization length, especially dealing with the case of non-linear behaviors of the materials.

When the strain is lower than $\varepsilon = 0.5\%$ (Point Q1 in Figure 4), the strain field is nearly homogeneous, and there is no localization bands observed. However, the strain level increases denoting a possible diffuse and homogeneous first step phase transformation (see Figure 3.a).

When the average strain bypass 1% (Point Q2), the first localization band appears. This localization band enlarges when the mean strain increases (between Point Q2 and Q3) (Figure 3.b). When the mean strain value reaches 2.7%, a secondary localization band appears (see Figure 3.c). At several points, the local strain values are nearly close to zero. These points may correspond to large but ill-oriented grains with respect to the tensile direction.

Localization bands form an angle of $\theta = 50.6^\circ$. This result is consistent with the localization theory [J.W.Rudnicki and J.R.Rice (1975) and J.R.Rice et al. (1979)].

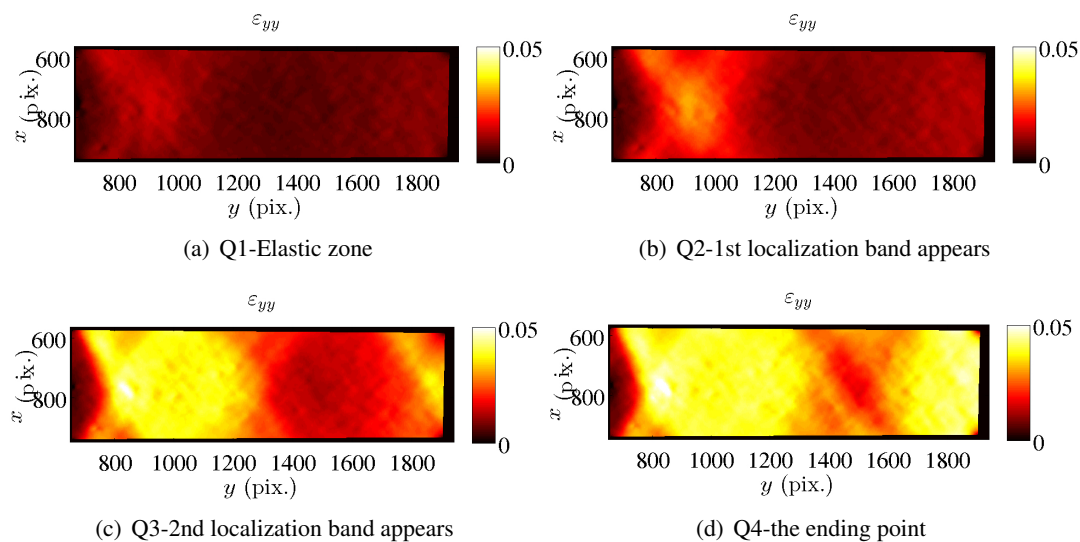


Figure 3: The evolution of the strain field at different points for quasi-static tensile loading $\dot{\varepsilon} = 2.5 \times 10^{-4} \text{ s}^{-1}$

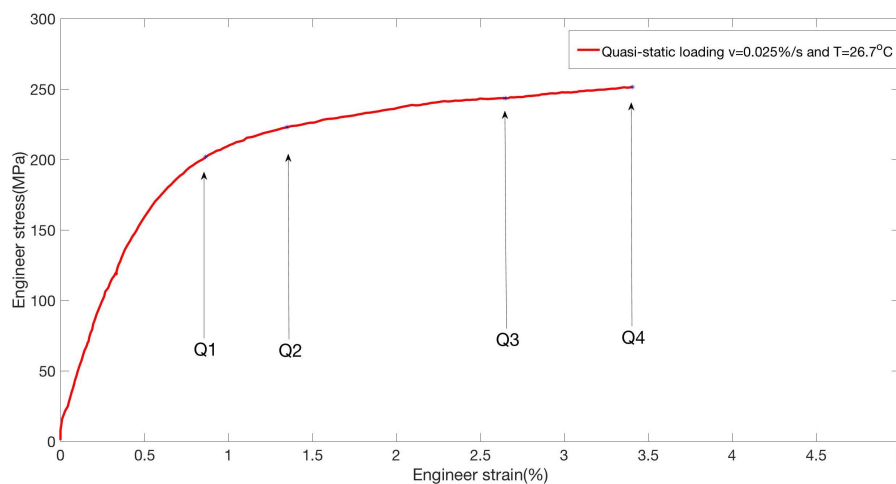


Figure 4: Stress strain curve at room temperature

Conclusions

Regularization Digital Images Correlation has been shown to be a powerful tool to capture the strain field in situation where the classical Digital Images Correlation fails (small size sample). This technique has been proven on the other hand to consume less computation time. It has been applied in this work to the observation of nucleation and propagation of strain localization bands in NiTi SMA .

These measurements must be complemented by X-ray measurement to estimate the *austenite*, *martensite* and *R*-phase ratio that are associated with. A connection between phase ratio and strain localization will be looked for.

References

- F. Hild and S. Roux. Comparaison of local and global approaches to digital images correlation. *Exp. Mech*, 52(9):1503–1519, 2012.
- J.R.Rice, J.W.Rudnicki, et al. A note on some features of the theory of localization of deformation. *Int. J. Solids Structures*, 16:597–605, 1979.
- J.W.Rudnicki and J.R.Rice. Condition for the localization of deformation in pressure-sensitive dilatant materials. *J.Mech.Phy.Solids*, 23:371–394, 1975.
- A. Maynadier, K. Lavernhe-Taillard, and O. Hubert. Thermomechanical modelling of a NiTi SMA sample submitted to displacement-controlled tensile test. *International Journal of Solids and Structures*, 51:1901–1922, 2014.
- Q. Sun and Y. He. A multiscale continuum model of the grain-size dependence of stress hysteresis in shape memory alloy polycrystals. *International Journal of Solids and Structures*, 45:330–343, 2008.
- T. Zvonimir, F. Hild, and S. Roux. Mechanical-aided Digital Images Correlation. *Strain Analysis*, 48: 330–343, 2013.